LA-UR-22-31798

Approved for public release; distribution is unlimited.

Title:	Actinide (III/IV) - Silica Colloids in the WIPP
Author(s):	Beam, Jeremiah Cooper
Intended for:	Report
Issued:	2022-11-07

Los Alamos
NATIONAL LABORATORY







Los Alamos National Laboratory, an affirmative action/equal opportunity employer, is operated by Triad National Security, LLC for the National Nuclear Security Administration of U.S. Department of Energy under contract 89233218CNA000001. By approving this article, the publisher recognizes that the U.S. Government retains nonexclusive, royalty-free license to publish or reproduce the published form of this contribution, or to allow others to do so, for U.S. Government purposes. Los Alamos National Laboratory requests that the publisher identify this article as work performed under the auspices of the U.S. Department of Energy. Los Alamos National Laboratory strongly supports academic freedom and a researcher's right to publish; as an institution, however, the Laboratory does not endorse the viewpoint of a publication or guarantee its technical correctness.

NOTICE: The current controlled version of this document is on the LCODocs website (http://lcodocs.lanl.gov/). A printed copy of the document may not be the current version.

LOS ALAMOS NATIONAL LABORATORY
CARLSBAD OPERATIONS
LCO-ACP-27, REVISION 0

Actinide (III/IV) - Silica Colloids in the WIPP

Jeremiah C. Beam

Effective Date: _____

Originator:

_____ _____
Jeremiah Beam, LANL-CO ACRSP Date

Technically Reviewed by:

_____ _____
Ugras Kaplan, LANL-CO ACRSP Date

Approved by:

_____ _____
Jeremiah Beam, LANL-CO ACRSP Team Leader Date

_____ _____
Priscilla Yanez, LANL-CO Quality Assurance Manager Date

_____ _____
Douglas Weaver, WIPP/RSO Program Director Date

History of Revision/Change

Revision Number	Effective Date	Pages Affected	Description of Revision
0		All	Original Release

Table of Contents

Section		Page
1.0	Purpose	1
2.0	Quality Assurance, References, Acronyms, and Definitions	1
2.1	Quality Assurance	1
2.2	References	1
2.3	Acronyms and Definitions	2
3.0	Introduction	3
4.0	Experimental Description	4
5.0	Results and Discussion	6
5.1	Nd(III)-Silica System	6
5.2	U(IV)-Silica System	8
6.0	Conclusion	10
Appendix 1	ICP-MS Tables	11

Table of Figures

Figure	Page
Figure 1. XRD Pattern of $Nd(OH)_3$	6
Figure 2. Nd(III) solubility in 5 M NaCl as a function of pH.	7
Figure 3. Nd(III) solubility in the presence of silicate in 5 M NaCl.	8
Figure 4. Solubility of U(IV) in 5 M NaCl as a function of pH.	9
Figure 5. Solubility of U(IV) in the presence of silicate in 5 M NaCl.	10

1.0 Purpose

During the completeness process for the 2019 Compliance Recertification Application (CRA) for the Waste Isolation Pilot Plant (WIPP), the US Environmental Protection Agency (EPA) raised concerns about the possible presence of actinide-silica colloids in the WIPP. Several publications that studied the An(IV)-silica system indicated that these colloids could form under conditions similar to WIPP. Colloids are important for WIPP Performance Assessment (PA) as these are a mobile fraction of actinides that contribute to release. As the previously published papers did not explore the formation of actinide-silica colloids under the high ionic strength environment expected in WIPP, an experimental strategy to study these systems was developed.

2.0 Quality Assurance, References, Acronyms, and Definitions

2.1 Quality Assurance

This work was compliant with the LANL-CO Quality Assurance (QA) Program. All experimental procedures and data analysis are included in scientific notebook JCB-2, issued to Jeremy Beam as a Developmental Notebook for Actinide Colloid Studies. Data collection was performed as outlined in QA approved procedures.

2.2 References

Domski, P.S.; Sisk-Scott, C. 2019. Prediction of Baseline Actinide Solubilities for CRA 2019 with an Updated EQ3/6 Pitzer Thermodynamic Database, DATA0.FM4. Sandia National Laboratories, Carlsbad, NM. ERMS 571178.

Dreissig, I.; Weiss, S.; Hennig, C.; Bernhard, G.; Zänker, H. 2011. Formation of Uranium(IV)-Silica Colloids at Near-Neutral pH. Geochimica et Cosmochimica Acta. 75, 352-367.

Hennig, C.; Weiss, S.; Banerjee, D.; Brendler, E.; Honkimäki, V.; Cuello, G.; Ikeda-Ohno, A.; Scheinost, A.C.; Zänker, H. 2013. Solid-state properties and colloidal stability of thorium(IV)-silica nanoparticles. Geochimica et Cosmochimica Acta. 103, 197-212.

Husar, R.; Weiss, R; Hennig, C.; Hübner, R.; Ikeda-Ohno, A.; Zänker, H. 2015. Formation of Neptunium(IV)-Silica Colloids at Near-Neutral and SIlightly Alkaline pH. Environmental Science and Technology. 49, 665-671.

Neill, T.S.; Morris, K.; Pearce, C.I.; Sherriff, N.K.; Burke, M.G.; Chate, P.A.; Janssen, A.; Natrajan, L.; Shaw, S. 2018. Stability, Composition, and Core-Shell Particle Structure of Uranium(IV)-Silicate Colloids. *Environmental Science and Technology.* 52, 9118-9127.

Peretroukhine, V.; Riglet-Martial, C.; Capdevila, H.; Calmon, V.; Bienvenu, P.; Laszak, I. 2002. Effect of Soluble Silicates on the Solubility of Thorium(IV) Hydrous Oxide. J. Nuclear Science and Technology. Supp 3, 516-519.

Rai, D.; Yui, M.; Moore, D.A.; Lumetta, G.J.; Rosso, M.K.; Xia, Y.; Felmy, A.R.; Skomurski, F.N. 2008. Thermodynamic Model for ThO_2(am) Solubility in Alkaline Silica Solutions. *Journal of Solution Chemistry.* 37, 1725-1746.

U.S. DOE. 2019. Title 40 CFR Part 191 Compliance Recertification Application for the Waste Isolation Pilot Plant. Carlsbad, NM. Carlsbad Field Office. DOE/WIPP-19-3609, Rev. 0.

U.S. EPA. 2022. Technical Support Document for 194.24. Evaluation of the Compliance Recertification Application (CRA-2019) Actinide Source Term, Gas Generation, Backfill Efficacy, Water Balance, and Cuelbra Dolomite Distribution Coefficient Values.

Van Soest, G. Performance Assessment Inventory Report – 2018. 2018. Los Alamos National Laboratory. Carlsbad, NM. LA-UR-18-31882.

Zänker, H.; Weiss, S.; Hennig, C.; Brendler, V.; Ikeda-Ohno, A. 2016. Oxyhydroxy Silicate Colloids: A New Type of Waterborne Actinide(IV) Colloids. Chemistry Open Reviews. 5, 174-182.

2.3 Acronyms and Definitions

Am(III)	Americium in the +III oxidation state
An(III)	Actinide in the +III oxidation state
An(IV)	Actinide in the +IV oxidation state
CRA	Compliance recertification application
DBR	Direct brine release
DOE	United States Department of Energy
EPA	United States Environmental Protection Agency
HPW	High purity water
HQ	Hydroquinone
ICP-MS	Inductively Coupled Plasma-Mass Spectroscopy
K	One thousand
kDa	Kilodalton
M	Molarity (moles of solute per liter of solvent)
mM	Millmolar (10^{-3} moles of solute per liter of solvent)
Nd(III)	Neodymium in the +III oxidation state
Nm	Nanometers
Np(IV)	Neptunium in the +IV oxidation state
pH	negative log of the hydrogen ion concentration

pC_{H+}	negative log of the hydrogen ion activity
Pu(III)	Plutonium in the +III oxidation state
Pu(IV)	Plutonium in the +IV oxidation state
RPM	Revolutions per minute
SiO_2	Silica
$Si(OH)_4$	Silicic acid, or silicate
Th(IV)	Thorium in the +IV oxidation state
TMOS	Tetramethylorthosilicate
TSD	Technical support document
U(IV)	Uranium in the +IV oxidation state
U(VI)	Uranium in the +VI oxidation state
UV-vis	Ultraviolet-visible spectroscopy

3.0 Introduction

Silica (SiO_2) is a prevalent component of waste emplaced at the WIPP. Laboratory equipment such as pipettes and glassware are usually manufactured from borosilicate glass. Silica is also present in soils that may be contained in legacy waste and in concrete emplacement materials. The estimated mass of soil (anticipated and emplaced) scaled to a full repository in the WIPP is 5.01×10^6 kg (Van Soest 2018). In direct brine release (DBR) scenarios, the alkaline brine can easily dissolve these silicate materials and introduce significant amounts of aqueous silica. In the technical support documents for the most recent compliance recertification application (US DOE 2019), the EPA expressed an interest in the possible presence of actinide-silica colloids in the WIPP repository (US EPA 2022). Recent studies have shown that aqueous silica can form colloidal species with actinides and actinide analogs. In WIPP PA calculations, this can lead to increased mobility of intrinsic and mineral fragment actinide colloids. Intrinisc colloids are operationally defined as colloids that are between 2.5-10 nm in size, whereas mineral colloids are operationally defined as colloids that are between 10-450 nm.

The effects of soluble silicates on the solubility of $ThO_2 \cdot xH_2O$ was first investigated at near-neutral to alkaline pH (6-12) in 0.1 M $NaClO_4$ (Peretroukhine, et al. 2002). A near-linear increase in dissolved thorium concentration was observed with the addition of silicate.

The solid-state properties and stability of the thorium(IV)-silica system were further studied (Hennig, et al. 2013). Th(IV)-silica colloids were prepared through the dilution of $Th(CO_3)_5^{6-}$ with stock solutions of hydrolyzed tetramethylorthosilicate (TMOS), which produces monosilicic acid [$Si(OH)_4$]. The preparation of these colloids produced aqueous Th(IV) concentrations of up to 1×10^{-3} M. At silicate concentrations below 1 mM, sedimentation of the Th(IV) solids occurred and no colloid formation was observed. These sedimented solids could not be resuspended in silicate solution to produce Th(IV)-silica colloids.

A similar route of synthesis was found for U(IV)-silica colloids (Neill, et al. 2018). U(IV)-carbonate complexes were synthesized and diluted with solutions of sodium metasilicate. The final silicate concentrations were in the range of 0-4 mM. These studies also included the alkaline pH range (6-12), however, colloid formation wasn't observed at pH values greater than 9 and silica concentrations less than 2 mM. The resulting colloids had a core-shell type structure, with a uraninite (UO_2) core, surrounded by a disordered silicate shell. Through centrifugation and filtration with Pall Nanosep filters, they found that most of these colloids were < 12 nm in size. Pall Nanosep filters of sizes 300, 100, 10, and 3 kDa were correlated to colloid sizes of 12, 7, 3, and 1.5 nm, respectively. In U(VI)-silica control experiments, no colloids were shown to form (Dreissig, et al. 2011)

The ability of Np(IV) to form colloids with silica has been observed at mildly alkaline pH (up to 8.5) using silicic acid as the silicate source (Husar, et al. 2015). Np(IV)-carbonate complexes were diluted with carbonate containing solutions, similarly to the Th(IV) and U(IV) systems. 80% of these colloids were found to be between 2-250 nm by a combination of filtration techniques. If that silica concentration was below 2 mM, colloids were not formed until the pH was reduced below 8.5 using 0.1 M nitric acid.

In all previous studies, colloids were only formed through the dilution of An(IV)-carbonate complexes with silicic acid solutions. This is in stark contrast to the WIPP system, which is modeled from an undersaturation viewpoint. When a DBR occurs, brine inundates the repository and the solids contained in the waste come into equilibrium with the brine and other dissolved waste components. In this situation, An(IV)-carbonate complexes are not expected to predominate under the alkaline (pH 9.5), high ionic strength (>5 M) environment. Hydroxide or hydroxycarbonate An(IV) species are expected to make up 100% of the dissolved actinide species under these conditions (Domski and Sisk-Scott 2019). For the An(III) system, hydroxide complexation accounts for roughly 90% of dissolved An(III), with the remaining 10% accounted for by organic ligand complexation. To simulate experimental conditions predicted to occur in WIPP, experiments starting from undersaturation are more appropriate.

As the colloidal behavior of thorium is quite unique among the +IV actinides, U(IV) was chosen as an analog to the behavior of Pu(IV), which is the most important +IV actinide for calculating release. While Pu(IV) can be difficult to maintain in solution, U(IV) can be maintained in aqueous systems using a reductant. The most common reductants used are Fe metal and $SnCl_2$. As metal-colloid formation was being studied in this system, an organic reductant, hydroquinone, was used to eliminate any possible competition for silica complexation in solution. The An(III)-silica system, which has not been previously studied, will use neodymium as an analog for both Am(III) and Pu(III), the two most important +III actinides for release calculations.

4.0 Experimental Description

$Nd(OH)_3$ was synthesized by dissolving 1.9210 g $NdCl_3 \cdot 6H_2O$ (Sigma-Aldrich, lot# MKCH0593) in 10 mL high purity water (HPW, 18.2 MΩ) and adding 50% sodium hydroxide (Acros Organics, lot# A0277324) dropwise to a pH of 10 in a nitrogen glovebox. Powder X-ray Diffraction (XRD) analysis confirmed the structure of the solid (Figure 1).

$U(OH)_4$ was synthesized by dissolving 0.5 g UCl_4 in 10 mL 1 M HCl (Fisher Scientific, lot# 4217070) in a nitrogen glovebox. This solution was analyzed by Ultraviolet-visible spectroscopy (UV-vis) to confirm the

U(IV) oxidation state. An aliquot of this uranium solution was added directly to a polypropylene bottle that had been equilibrated with brine for 2 weeks. 50% sodium hydroxide (Acros organics, lot# A0277324) was added to this solution to precipitate $U(OH)_4$.

5 M NaCl was prepared by first degassing 1.1 L of HPW with nitrogen for 5 hours. This water was placed into a glovebox, where 242 g of NaCl (Fisher Scientific, lot # 212333) was added to 800 mL of HPW. HPW was added to completely dissolve the NaCl and the total volume was brough to 1 L using a volumetric flask (Corning, lot, VF-34). This solution was then filtered using a 0.2 µm nylon Nalgene Rapid Flow Filter unit. A sample of this brine was taken, and Inductively Coupled Plasma-Mass Spectroscopy (ICP-MS) analysis was performed to confirm the concentration according to procedure ACP-EXP-11, rev. 5 (Inductively Couple Plasma-Mass Spectrometry).

20 mL of the previously prepared 5M NaCl was added to the uranium and neodymium solids along with 133 µL of a previously prepared $NaSiO_3 \cdot 9H_2O$ (Acros Organics, lot #A0401412) solution (2.8266 g dissolved in 15.4 mL HPW) giving a final concentration of 4 mM silica. The pH adjustments were made using 1 M HCl and carbonate free 50% NaOH to achieve pC_{H+} values of 2, 4, 6, 8, and 10. The measured pH values were corrected for ionic strength to pC_{H+} according to procedure ACP-EXP-010, rev. 2 (Determination of Hydrogen Ion Concentration in Brine). Hydroquinone (Acros Organics, lot #A0415861) was added to the U(IV) experiments to maintain redox control and prevent the formation of U(VI).

The samples were prepared and stored in a nitrogen glovebox where constant monitoring ensured an oxygen concentration of less than 5 ppm. A 500 µL aliquot from each experiment was taken and filtered using a 30 kDa Pall Nanosep filter and centrifuged at 13K RPM for 30 minutes. A 100 µL aliquot of this filtrate was dissolved into 900 uL 2% HNO_3 (Fisher Scientific, lot# 1221080) to create a 1:10 dilution. The remaining 400 µL of filtrate was then added to a 10 kDa Pall Nanosep filter and centrifuged at 13K for 30 minutes. 100 µL of this filtrate was then added to 900 µL of 2% HNO_3 to create a 1:10 stock solution. The remaining 300 µL was then added to a 3 kDa Pall Nanosep filter and centrifuged at 13.4K RPM for 1 hour. 100 µL of this filtrate was then added to 900 µL of 2% HNO_3 to create a 1:10 dilution. Lastly, a 500 µL aliquot from each experiment was added to a 3 kDa Pall Nanosep filter and centrifuged at 13.4K RPM for 1 hour. 100 µL of this filtrate was then added to 900 µL of 2% HNO_3 to generate a 1:10 dilution.

100 µL from each 1:10 dilution was added to 1700 µL of 2% HNO_3 (Fisher Scientific, lot # 1218110) with 300 ppb of an indium internal standard (High Purity Standards, lot# 2013216) to provide a final dilution of 1:180 in duplicate for ICP-MS analysis.

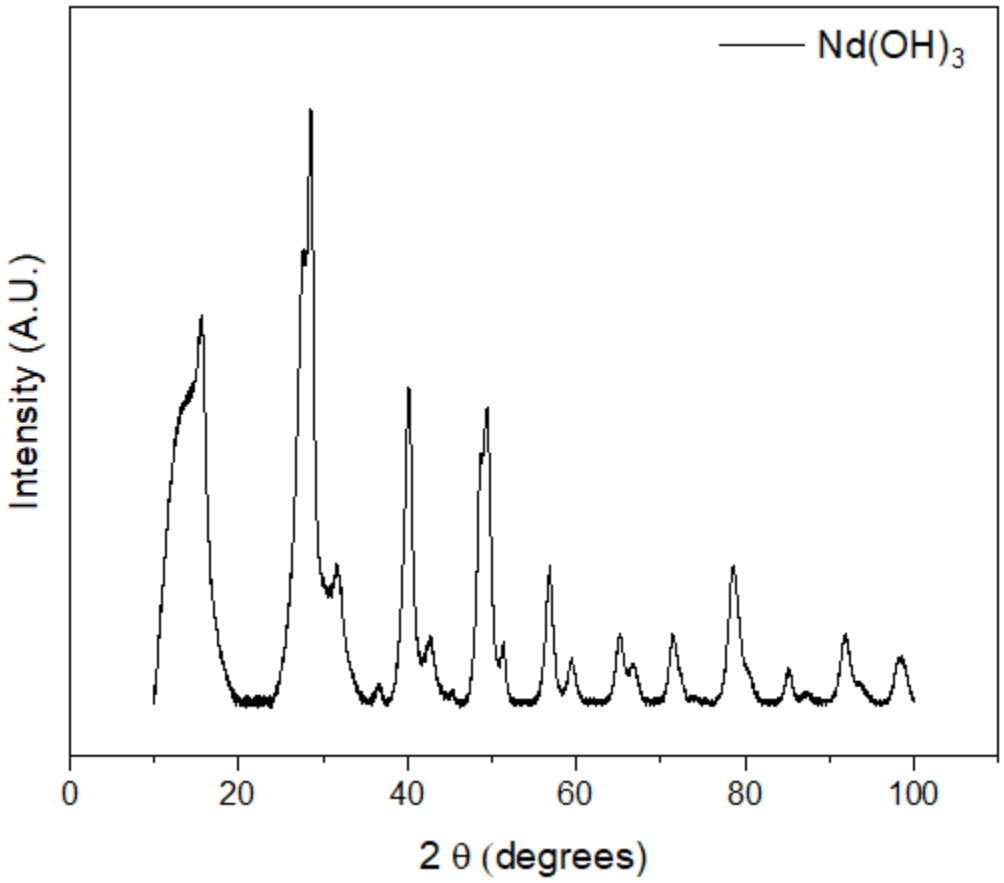


Figure 1. XRD pattern of $Nd(OH)_3$.

5.0 Results and Discussion

5.1 Nd(III)-Silica System

Nd(III) solubility in 5 M NaCl as a function of pH is shown in Figure 2. There is slight drift from the targeted pC_{H+} values of 2, 4, 6, 8, and 10 due to the lack of any buffering by NaCl solutions. A small volume addition or acid or base can result in a large pH shift in the solution. The solubility remains high until around pH 8.5, where a drastic decrease in solubility occurs. This is due to the complete hydrolysis of Nd(III) aqueous species to form $Nd(OH)_3$, which is the solubility controlling phase under these conditions. In the presence of dissolved silicate (Figure 3), this trend remains the same, indicating that hydrolysis is a stronger force than silicate complexation under these conditions. Sequential filtration of these samples does not indicate the presence of Nd-silica colloids, as the solubility trend remains the same as without silicate present.

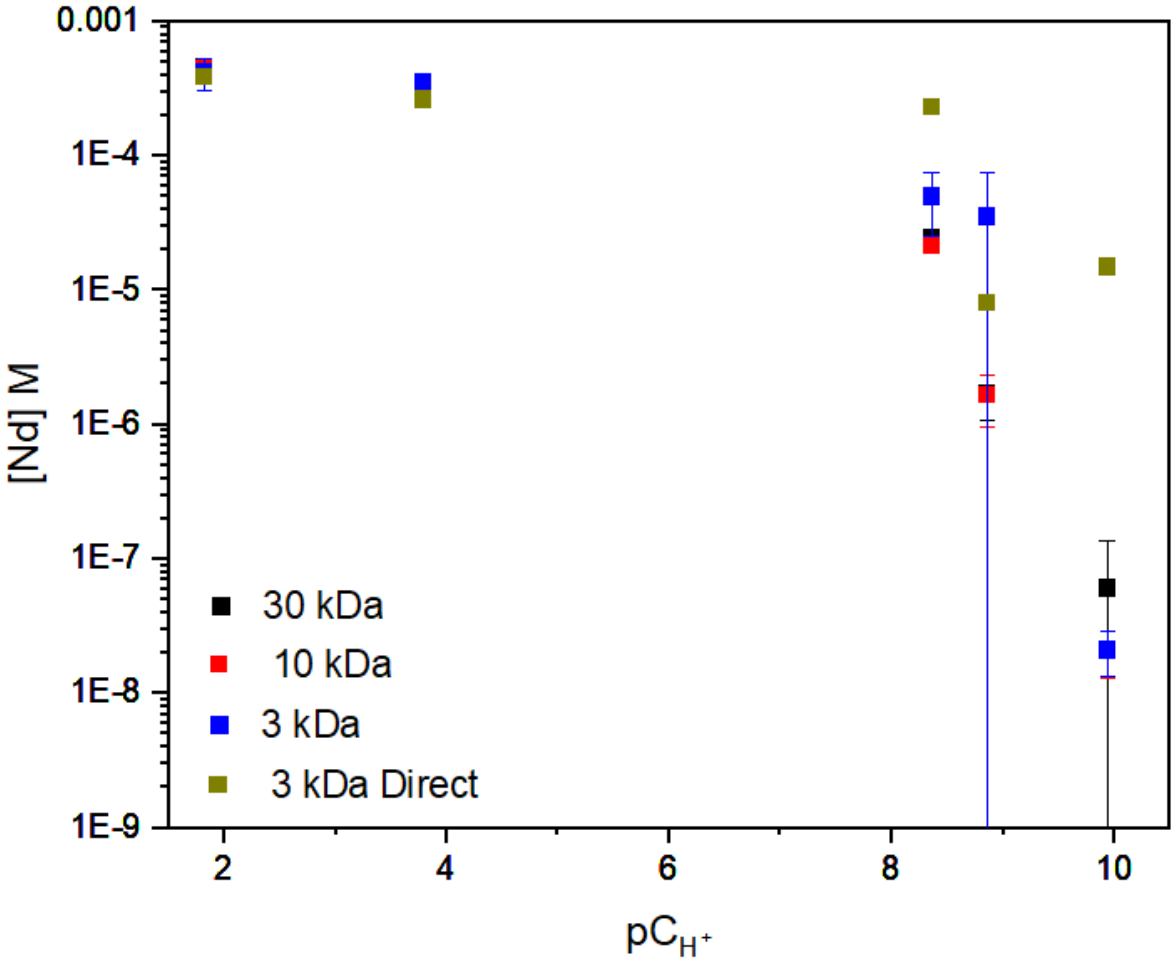


Figure 2. Nd(III) solubility in 5 M NaCl as a function of pH.

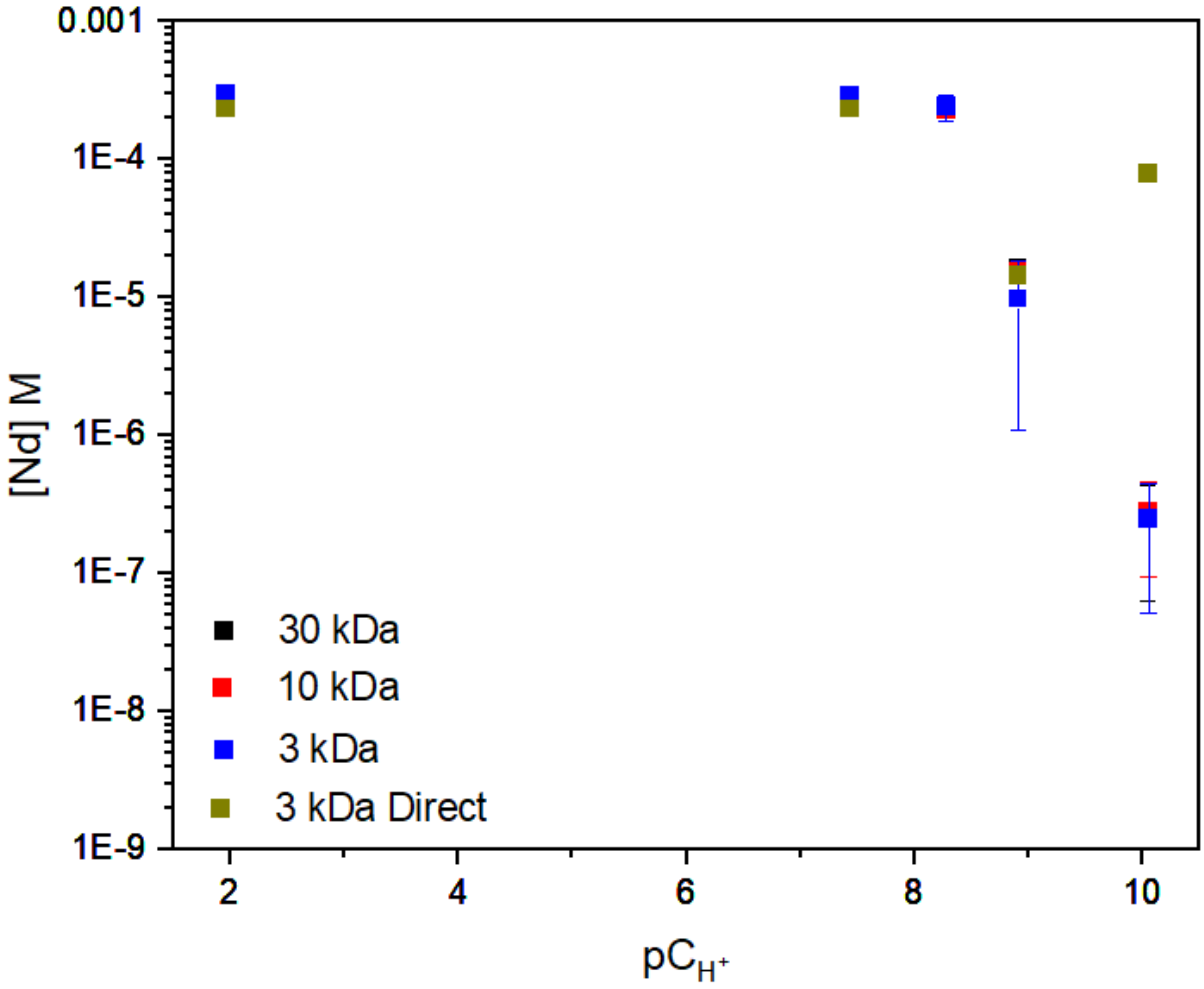


Figure 3. Nd(III) solubility in the presence of silicate in 5 M NaCl.

5.2 U(IV)-Silica System

The U(IV) solubility in 5 M NaCl as a function of pH is shown in Figure 4. The solubility trend is similar to that of Nd(III), however the rapid decrease in solubility as pH increases occurs around pH 8, indicating that hydrolysis of U(IV) is stronger than Nd(III). A slight increase in solubility occurs around pH 10 in the presence of silica (Figure 5), which is consistent with the formation of $An(OH)(H_3SiO_4)_3^{2-}$, which has previously been reported for Th (Rai, et al. 2008). This species should not be important to WIPP PA calculations, as it does not become predominate until pH > 10. The WIPP is buffered to pH 9.5 due to the presence of MgO stacked on top of the waste, which will remove carbonate from solution.

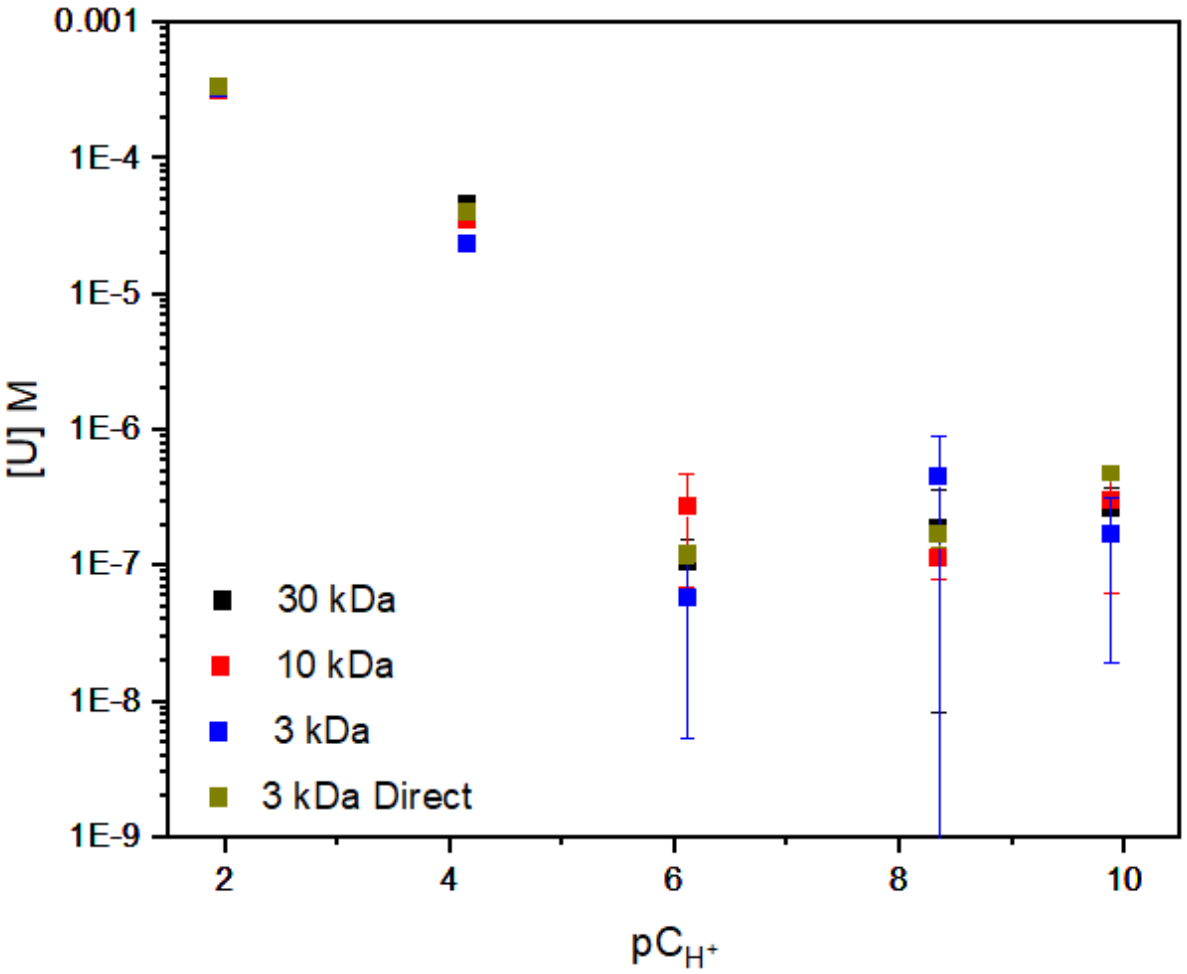


Figure 4. Solubility of U(IV) in 5 M NaCl as a function of pH.

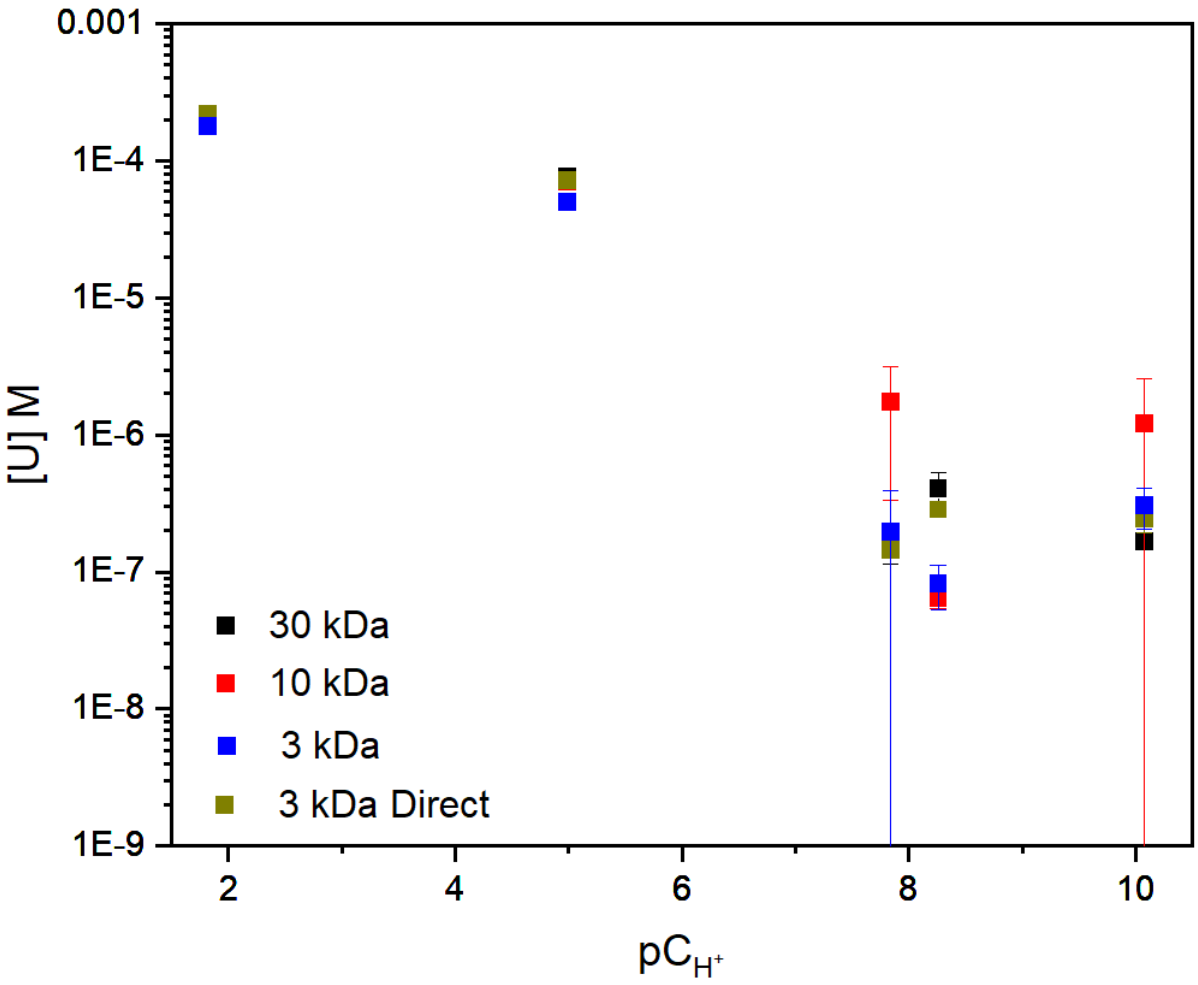


Figure 5. Solubility of U(IV) in the presence of silicate in 5 M NaCl.

6.0 Conclusion

The effect of dissolved silica on the solubility of An(III) and An(IV) solids, as well as the possibility of actinide-silica colloids was studied in 5 M NaCl solutions. At pH values relevant to WIPP, no significant colloid fraction was observed by sequential filtration. Additionally, no increase in solubility was observed in the presence of dissolve silica. This indicates that actinide-silica colloids do not form under conditions that simulate a DBR into the repository. Additionally, as there is no effect on the solubility, incorporation of silicate speciation, complexation, and aqueous chemistry into the WIPP model would have no impact on release calculations.

Appendix 1. ICP-MS Data for Nd(III)-silica colloid experiments

First Sampling, without silicate

pH	30 K [Nd] M	10 K [Nd] M	3 K [Nd] M	3 K direct [Nd] M
1.82	$2.540\times10^{-4} \pm 5.680\times10^{-6}$	$2.5512\times10^{-4} \pm 2.469\times10^{-5}$	$2.531\times10^{-4} \pm 3.469\times10^{-5}$	$2.466\times10^{-4} \pm 1.276\times10^{-6}$
3.79	$2.593\times10^{-4} \pm 4.421\times10^{-6}$		$2.660\times10^{-4} \pm 1.863\times10^{-5}$	$2.620\times10^{-4} \pm 3.804\times10^{-6}$
8.36	$2.291\times10^{-4} \pm 7.958\times10^{-6}$	$2.628\times10^{-4} \pm 3.199\times10^{-5}$	$2.170\times10^{-4} \pm 2.1807\times10^{-5}$	$2.354\times10^{-4} \pm 1.706\times10^{-6}$
8.86	$1.021\times10^{-5} \pm 8.7358\times10^{-7}$	$1.077\times10^{-5} \pm 5.335\times10^{-7}$	$7.328\times10^{-6} \pm 4.5539\times10^{-7}$	$1.110\times10^{-5} \pm 1.379\times10^{-6}$
9.94	$1.904\times10^{-7} \pm 1.831\times10^{-7}$	$1.015\times10^{-6} \pm 1.000\times10^{-7}$	$1.83610^{-7} \pm 2.208\times10^{-7}$	$7.225\times10^{-8} \pm 2.665\times10^{-8}$

First Sampling, with silicate

pH	30 K [Nd] M	10 K [Nd] M	3 K [Nd] M	3 K direct [Nd] M
1.96	$4.276\times10^{-4} \pm 8.252\times10^{-6}$	$4.349\times10^{-4} \pm 1.428\times10^{-5}$	$4.601\times10^{-4} \pm 9.130\times10^{-6}$	$4.1073\times10^{-4} \pm 1.332\times10^{-5}$
7.43	$2.685\times10^{-4} \pm 4.366\times10^{-6}$		$2.686\times10^{-4} \pm 2.686\times10^{-4}$	$1.682\times10^{-4} \pm 7.140\times10^{-6}$
8.28	$1.603\times10^{-5} \pm 6.530\times10^{-7}$		$1.523\times10^{-5} \pm 7.612\times10^{-7}$	$1.534\times10^{-5} \pm 6.680\times10^{-8}$
8.91	$1.051\times10^{-6} \pm 8.681\times10^{-7}$	$1.503\times10^{-7} \pm 3.0546\times10^{-8}$	$2.075\times10^{-7} \pm 4.894\times10^{-7}$	$3.910\times10^{-7} \pm 3.424\times10^{-8}$
10.05	$1.870\times10^{-7} \pm 1.113\times10^{-7}$	$8.8671\times10^{-7} \pm 3.196\times10^{-8}$	$2.711\times10^{-7} \pm 4.894\times10^{-7}$	$3.180\times10^{-7} \pm 6.442\times10^{-9}$

Second Sampling, without silicate

pH	30 K [Nd] M	10 K [Nd] M	3 K [Nd] M	3 K direct [Nd] M
1.82	$2.715\times10^{-4} \pm 3.729\times10^{-6}$	$2.666\times10^{-4} \pm 1.776\times10^{-6}$	$3.264\times10^{-4} \pm 5.923\times10^{-6}$	$3.017\times10^{-4} \pm 3.498\times10^{-5}$
3.79	$2.619\times10^{-4} \pm 4.874\times10^{-6}$	$2.953\times10^{-4} \pm 5.298\times10^{-5}$	$3.277\times10^{-4} \pm 4.561\times10^{-6}$	$3.107\times10^{-4} \pm 4.470\times10^{-7}$
8.36	$2.349\times10^{-4} \pm 2.323\times10^{-6}$	$2.394\times10^{-4} \pm 5.829\times10^{-6}$	$3.067\times10^{-4} \pm 5.673\times10^{-6}$	$2.641\times10^{-4} \pm 1.960\times10^{-6}$
8.86	$9.152\times10^{-6} \pm 2.056\times10^{-7}$	$8.505\times10^{-6} \pm 5.2832\times10^{-7}$	$9.7588\times10^{-6} \pm 1.739\times10^{-7}$	$1.183\times10^{-5} \pm 4.071\times10^{-8}$
9.94		$3.125\times10^{-8} \pm 6.0083\times10^{-9}$	$1.982\times10^{-8} \pm 7.451\times10^{-9}$	$6.4911\times10^{-8} \pm 6.538\times10^{-9}$

Second Sampling, with silicate

pH	30 K [Nd] M	10 K [Nd] M	3 K [Nd] M	3 K direct [Nd] M
1.96	$4.649x10^{-4} \pm 5.217x10^{-6}$	$4.649x10^{-4} \pm 2.339x10^{-6}$	$5.883x10^{-4} \pm 6.016x10^{-6}$	$4.819x10^{-4} \pm 1.516x10^{-6}$
7.43	$3.375x10^{-4} \pm 3.149x10^{-6}$	$3.260x10^{-4} \pm 2.486x10^{-6}$	$4.262x10^{-4} \pm 4.877x10^{-6}$	$3.793x10^{-4} \pm 6.812x10^{-6}$
8.28	$2.432x10^{-5} \pm 3.088x10^{-7}$	$2.244x10^{-6} \pm 5.653x10^{-7}$	$2.840x10^{-5} \pm 5.128x10^{-7}$	$2.759x10^{-6} \pm 3.449x10^{-7}$
8.91		$8.889x10^{-8} \pm 6.653x10^{-9}$	$1.344x10^{-7} \pm 4.449x10^{-8}$	$1.230x10^{-7} \pm 1.3081x10^{-9}$
10.05		$1.970x10^{-8} \pm 3.527x10^{-9}$	$6.362x10^{-8} \pm 2.940x10^{-8}$	$6.4726x10^{-9} \pm 1.482x10^{-9}$

Third Sampling, without silicate

pH	30 K [Nd] M	10 K [Nd] M	3 K [Nd] M	3 K direct [Nd] M
1.82	$4.574x10^{-4} \pm 3.706x10^{-6}$	$4.471x10^{-4} \pm 4.366x10^{-6}$	$4.141x10^{-4} \pm 1.062x10^{-4}$	$3.833x10^{-4} \pm 2.6624x10^{-7}$
3.79	$3.520x10^{-4} \pm 4.178x10^{-6}$	$3.282x10^{-4} \pm 1.553x10^{-6}$	$6.504x10^{-4} \pm 1.7087x10^{-5}$	$2.625x10^{-4} \pm 3.666x10^{-6}$
8.36	$2.416x10^{-5} \pm 1.292x10^{-6}$	$2.1257x10^{-6} \pm 2.389x10^{-6}$	$5.002x10^{-5} \pm 2.458x10^{-5}$	$2.290x10^{-4} \pm 5.000x10^{-6}$
8.86	$1.706x10^{-6} \pm 6.353x10^{-7}$	$1.651x10^{-6} \pm 6.914x10^{-7}$	$3.519x10^{-5} \pm 3.9474x10^{-6}$	$8.005x10^{-6} \pm 2.654x10^{-7}$
9.94	$6.090x10^{-8} \pm 7.526x10^{-8}$	$2.090x10^{-8} \pm 7.7588x10^{-9}$	$2.090x10^{-8} \pm 7.708x10^{-9}$	$1.484x10^{-6} \pm 6.939x10^{-8}$

Third Sampling, with silicate

pH	30 K [Nd] M	10 K [Nd] M	3 K [Nd] M	3 K direct [Nd] M
1.96	$2.740x10^{-4} \pm 5.916x10^{-6}$	$2.619x10^{-4} \pm 8.370x10^{-6}$	$3.005x10^{-4} \pm 5.078x10^{-6}$	$2.3330x10^{-4} \pm 4.472x10^{-8}$
7.43	$2.594x10^{-4} \pm 1.068x10^{-5}$	$2.655x10^{-4} \pm 5.8633x10^{-6}$	$2.926x10^{-4} \pm 4.810x10^{-6}$	$2.320x10^{-4} \pm 8.080x10^{-7}$
8.28	$2.3652x10^{-5} \pm 1.647x10^{-5}$	$2.253x10^{-4} \pm 5.401x10^{-5}$	$2.428x10^{-5} \pm 5.401x10^{-5}$	
8.91	$1.619x10^{-5} \pm 1.291x10^{-6}$	$1.5572x10^{-5} \pm 1.651x10^{-6}$	$9.880x10^{-6} \pm 8.787x10^{-6}$	$1.445x10^{-6} \pm 2.092x10^{-7}$
10.05	$2.500x10^{-7} \pm 1.8652x10^{-7}$	$2.8011x10^{-7} \pm 1.865x10^{-7}$	$2.482x10^{-7} \pm 1.959x10^{-7}$	$7.956x10^{-5} \pm 1.870x10^{-7}$